American College of Neuropsychopharmacology

www.nature.com/npp

ARTICLE

Nucleus reuniens inactivation reverses stress-induced hypodopaminergic state and altered hippocampal-accumbens synaptic plasticity

Daniela L. Uliana[1]✉, Felipe V. Gomes[1,2] and Anthony A. Grace[1]

© The Author(s), under exclusive licence to American College of Neuropsychopharmacology 2022

The nucleus reuniens of the thalamus (RE) is a pivotal area responsible for the connectivity of the prefrontal-hippocampus pathway that regulates cognitive, executive, and fear learning processes. Recently, it was proposed that the RE participates in the pathophysiological states related to affective dysregulation. We investigated the role of RE in motivational behavioral and electrophysiological dysregulation induced by stress. Adult Sprague-Dawley rats were exposed to a combination of stressors (restraint stress+footshock) for 10 days and tested one to two weeks later in the forced swim test (FST), ventral tegmental area (VTA)dopamine (DA) neuron electrophysiological activity, and hippocampal-nucleus accumbens plasticity. The RE was inactivated by injecting TTX prior to the procedures. The stress exposure increased the immobility in the FST and decreased VTA DA neuron population activity. Whereas an early long-term potentiation (e-LTP) in the ventral hippocampus-nucleus accumbens pathway was found after fimbria high-frequency stimulation in naïve animals, stressed animals showed an early long-term depression (e-LTD). Inactivation of the RE reversed the stress-induced changes in the FST and restored dopaminergic activity. RE inactivation partially recovered the stress-induced abnormal hippocampal-accumbens plasticity observed in controls. Our findings support the role of the RE in regulating affective dysregulation and blunted VTA DA system function induced by stress. Also, it points to the hippocampal-accumbens pathway as a potential neural circuit through which RE could modulate activity. Therefore, RE may represent a key brain region involved in the neurobiology of amotivational states and may provide insights into circuit dysfunction and markers of the maladaptive stress response.

Neuropsychopharmacology (2022) 47:1513–1522; https://doi.org/10.1038/s41386-022-01333-1

INTRODUCTION

The nucleus reunions of the thalamus (RE) plays a critical role in the integration of frontocortical areas with the hippocampus (HIP) [1–5]. Impairments in hippocampal-prefrontal connectivity have long been described in psychiatric conditions [6–8]. For example, abnormal activation of frontal-hippocampal connectivity during negative valence stimulus processing and increased resting-state functional connectivity are found in patients with major depressive disorder (MDD) [9, 10]. Also, a decreased hippocampal volume [11] and impaired blood flow in the medial prefrontal cortex (mPFC) [12] are observed in MDD. Deficits in the mPFC-HIP connectivity have also been observed in rodent models for depression based on stress exposure [13]. Since the RE relays inputs from the mPFC to the HIP, disruptions in the activity of both the PFC and HIP and their connectivity may be related to the ability of the RE to integrate their activity. In fact, preclinical studies suggest that the RE is involved with affective regulation. Thus, lesion of the RE prevented the negative motivational impact induced by the chronic mild stress (CMS) model, which was accompanied by a decreased connectivity between mPFC-HIP [14]. Also, the RE lesion normalized the neuroanatomical atrophy in the mPFC and HIP induced by CMS [14, 15].

Stress-based protocols are extensively used in rodents to model circuit deficits associated with depression. Similar to what has been observed in depression patients [16–18], most of these protocols lead to anhedonia-like changes and blunted activity of the dopaminergic reward system [17, 19–23]. We recently found that the RE modulates dopamine (DA) neuron activity in the ventral tegmental area (VTA) [3]. The activation of the RE increases the number of spontaneous active VTA DA neurons in VTA through activation of the ventral HIP (vHIP). In addition, the increased dopaminergic activity induced by infralimbic PFC (iIPFC) inhibition, which also involves the vHIP [24], depends on RE activity [3], demonstrating its essential role in mPFC-HIP connectivity. This pathway represents a part of a larger circuit involved in the modulation of VTA and affective dysregulation [21, 25–27]. For example, the vHIP and its connectivity with nucleus accumbens (NAc) play an important role in regulating reward responses, dopaminergic activity in the VTA and susceptibility to stress [27–32]. Evidence suggest that stress-induced decreases in VTA DA system activity may be associated with abnormal vHIP-NAC connectivity [26]. This pathway could be under RE regulation considering its marked projections to the vHIP [33]. However, the role of the RE in the regulation of the

[1]Departments of Neuroscience, Psychiatry and Psychology, University of Pittsburgh, Pittsburgh, PA, USA. [2]Present address: Department of Pharmacology, Ribeirão Preto Medical School, University of São Paulo, Ribeirão Preto, SP, Brazil. ✉email: uliana@pitt.edu

Received: 8 October 2021 Revised: 11 March 2022 Accepted: 19 April 2022
Published online: 29 April 2022

hypodopaminergic state observed in amotivational states is still unexplored. Here, we investigated the impact of repeated stress exposure on VTA DA neuron activity and synaptic transmission in the vHIP-NAc pathway, and whether the inactivation of the RE circumvents stress-induced changes.

MATERIAL AND METHODS

Animals

Adult Sprague-Dawley male rats (post-natal day, PD58) obtained from Envigo (Indianapolis, IN) were housed in a temperature (22 ± 1 °C) and humidity-controlled room, with a 12 h/light-dark cycle and water/food available ad libidum. Male rats were used in this initial study given the marked difference in the impact of stress in males vs. females [23, 34–38]. The rats acclimated for 7 days prior to the stress procedure. The stress protocol, forced swim test, and electrophysiology were performed during the lights-on cycle. Behavior and electrophysiological procedure were carried out in accordance with the NIH Guide for the Care and Use of Laboratory Animals and approved by the Institutional Animal Care and Use Committee of the University of Pittsburgh.

Experimental design

The rats were subjected to a 10-day stress procedure or left undisturbed in the animal room facility (Naïve) between PD64-74. Electrophysiological measures and behavioral tests were done in an independent group of animals and were carried out between 1 and 2 weeks (PD81-88) after stress for all experimental designs [23]. Electrophysiological measures were distributed across the week (2 rats per day). For the FST, two-session within the week (PD82-83, 8–9 days after stress or PD86-87, 12–13 days after stress) were performed to match with the timeline of electrophysiological analysis. Correlational analysis showed no impact of the time of recording/behavior (across 1–2 weeks post-stress) on the results (Supplementary Fig. 1). In RE inactivation experiments, a cannula was implanted in the RE 1 day after the end of the stress protocol and the FST behavior was assessed at the same time-point described previously in two sessions. The RE cannulation in the electrophysiology experiments was carried out immediately before the physiology procedures.

Stress paradigm

A 10-days stress protocol was used to match our previous studies [23, 34, 39, 40]. The animals were subjected to a daily footshock (FS) session (25 FS, 1 mA/2 s, 20–60 s random interval) for 10 days. FS was combined with three sessions of 1 h restraint stress, in a Plexiglas cylindrical tube, with the procedure occurring on days 1, 2, and 10 immediately after the FS session.

RE cannula implantation

At the end of the stress protocol, the rats were returned to the animal care facility and a tablet of Rimadyl® was provided in the rat homecage (Bio-Serv; Carprofen 2 mg per tablet; 1 tablet each rat). 24 h later, rats were anesthetized with isoflurane and fixed in a stereotaxic frame. After incision and cleaning of the scalp, a stainless-steel guide cannula was implanted unliterally in the RE (anteroposterior: −2.3 mm from bregma; mediolateral: +2.3 mm from midline; ventral: −7.2 mm; angle 16°), using the Paxinos and Watson (1997) rat brain atlas as reference [41]. Acrylic cement and one metal screw were used to fix the cannula to the skull. A subcutaneous injection of Carprofen (5 mg/kg) was done by the end of the surgical procedure for analgesia. One day after surgery the rat received another carprofen tablet. The rats were allowed to recover for 7 days.

Forced swim test

A 2-day forced swim test (FST) procedure was started 1 week after the cannula implantation surgery. Naïve and stressed animals not implanted with cannula were also tested in the FST. The procedure was carried out using a Plexiglas cylinder (50 cm height; 20 cm diameter) filled with water (25 ± 1 °C) to a depth of 38-40 cm. On day one, each rat was subjected to forced swimming for 15 min. The next day (day 2), the rats were placed again in the water-filled cylinder and tested for 5 min. The time of immobility and latency to immobility were measured. Immobility was defined when the rat makes only the minimum necessary movements to maintain its head above the water [42, 43]. The water was changed between rats.

Electrophysiology

Electrophysiological recordings were performed 1–2 weeks post-stress. Rats received an intraperitoneal injection of chloral hydrate (400 mg/kg; i.p) and the anesthesia was maintained by additional injections (i.p) as needed to suppress the hindlimb compression reflex. The rats were fixed in a stereotaxic frame (Kopf) and the body temperature was maintained at 37 °C by a thermostatically-controlled heating pad (TR-200, F.S.T.). In vivo extracellular recordings were done using microelectrodes pulled from Omegadot 2.0 mm glass tubing on a vertical electrode puller (Narishige P-2) and the tip was broken under a microscopic. The glass electrode was filled with 2% Chicago Sky Blue dye in 2 M NaCl to yield an impedance of 6–16 MΩ. A preamplifier (2400A, Dagan) was used to amplified the signal (×1000) and filtered with open filter settings (low frequency cut off: 10 Hz; high frequency cut off: 30 kHz). The signal was displayed on an oscilloscope (PM3337, Philips) and transferred via Powerlab 8/30 interface (ADInstruments) to a computer with LabChart v.8 software. The cutoff used for analysis was >3 signal-to-noise ratio. Different animals were used to assess spontaneous dopamine neuron activity in the VTA and hippocampal-accumbens plasticity recordings.

For the recordings of VTA DA neurons, the electrode was lowered into the VTA (−5.3 mm posterior from bregma; 0.6 mm lateral to the midline and 6.5–9.0 mm ventral from the brain surface) and six to nine vertical tracks were sampled in a fixed pattern. Population activity (number of spontaneously active DA neurons per track), firing rate, and percentage of spikes occurring in bursts were the parameters analyzed. DA neuron identification was based on well-established electrophysiological characteristics [44, 45].

For evaluation of hippocampal-accumbens connectivity, the electrode was lowered into NAc shell (anteroposterior: +1.5–1.1 mm from bregma, mediolateral: +1.1–1.5 mm from the midline; ventral: −5.5–8 mm from the brain surface). For stimulation, concentric bipolar electrodes (NEX-100X; Rhodes Medical Instruments) targeted the fimbria (anteroposterior: −1.3 mm from bregma; mediolateral: −1.5 mm from the midline; ventral: 4.8 mm from the skull) for single-pulse and high-frequency stimulation (HFS; 20 Hz; 10 s at suprathreshold). A dual-output stimulator (S8800; Grass Technologies) was used to apply single-pulse stimulation to the fimbria (1 mA intensity/0.5 Hz frequency/0.25 ms pulse duration) in order to search for a responsive neuron in the NAc shell. The current intensity was adjusted to evoke an action potential approximately 50% of the time after a monosynaptically activated neuron was found. Monosynaptic connectivity was determined according to previous criteria [26, 46], which includes variability in latency to evoked spike discharge during the single-pulse stimulus baseline period. All the neurons recorded displayed spike durations >2 ms, characteristic of projection neurons [46]. The baseline spike probability was measured for 10 min before and after RE tetrodotoxin (TTX) injection. After HFS, neuron responsivity was measured for an additional 30 min. Spike probability was calculated by dividing the number of spikes by the total number of single-pulse stimuli and only one neuron in the NAc shell was recorded per animal. At the end of the recordings, the brains were removed for histological verification of stimulation, recording, and injection sites.

RE inactivation

The Na+ channel blocker, TTX, was used to evaluate the impact of inhibition of RE on behavior and electrophysiological responses. TTX was diluted in Dulbecco's PBS (dPBS; Sigma-Aldrich). TTX 1 M in 0.2 µL and dPBS (Veh; 0.2 µL) were delivered at a rate of 0.5 µl/min using a 2 µL Hamilton syringe (Hamilton, Co., USA) [3]. The infusion cannula (33 gauge) was used for the injection and was 1 mm longer than the guide cannula. The needles remained in place for 1 min after the injection to limit injection spread. In the behavioral experiment, TTX or Veh was infused into the RE 10 min before the FST on day 2. For electrophysiological recordings, TTX was administrated 10 min before recordings of VTA DA neurons or 10 min after monosynaptic connectivity evoked by fimbria stimulation in the NAc shell was found.

Histology

After the electrophysiological recordings, the localization of the electrode was evaluated by ejecting Chicago Blue dye with a constant negative current of −20 µA for 20 min. In the connectivity experiment, the location of the fimbria stimulating electrode was marked by delivering 10 s cathodal current at 200 µA. The brains were removed after decapitation and fixed in 8% paraformaldehyde solution for 48 h followed by 25% sucrose for cryoprotection. The brains were frozen after saturation and

sliced coronally (60 µm) using a cryostat (Leica Frigocut 2800). Brain sections containing the NAc, fimbria, RE, and VTA were displayed on gelatin-chormalum-coated slides and stained with neutral red and cresyl violet.

Statistical analysis

Data are presented as mean ± SEM. The experiments testing the impact of stress on the FST and VTA recordings were analyzed using *t*-test to compare naïve and stress conditions. For the experiments involving RE inactivation, two and/or three-way ANOVA were used with condition (Naïve × Stress) and treatment (Veh × TTX) as main factors, and time in case of repeated measures, followed by Tukey's posthoc test. Except for the data of VTA DA neurons burst activity in experiment 1 that was analyzed by the Mann-Whitney test and in experiment 2 by Kruskal-Wallis test since % burst data did not follow a normal distribution. The effect size was calculated for each experiment (Cohen's d for *t*-test and Cohen's *f* for ANOVA). A table showing the effect size and power values is presented in the Supplementary Table S1. $p < 0.05$ was defined as significant.

RESULTS

Stress increases immobility in the FST, causes a hypodopaminergic state in the VTA and long-term depression in the NAc shell induced by vHIP stimulation

Adult rats subjected to the repeated stress protocol were tested 1–2 weeks post-stress in the FST and VTA recordings (Fig. 1A). Stressed rats presented a decreased latency to immobility (Naïve, $n = 12$, 111.2 ± 7.94 s; Stress, $n = 12$, 66.17 ± 11.57 s; $t_{22} = 3.21$, $p = 0.0041$; $d = 1.31$; Fig. 1B) and increased time of immobility in the FST (Naïve, $n = 12$, 76.42 ± 6.66 s; Stress, $n = 12$, 109.4 ± 13.08 s; $t_{22} = 2.25$, $p = 0.035$; $d = 0.92$; Fig. 1C). Moreover, the adult stress decreased the number of spontaneously active VTA DA neurons (Naïve, $n = 7$ rats, 0.78 ± 0.06 cells/track; Stress, $n = 7$, 28 cells, 0.33 ± 0.08 cells/track; $t_{12} = 4.36$, $p = 0.0009$; $d = 2.33$; Fig. 1D) without changing the average firing rate (Naïve, 50 cells, 4.67 ± 0.29 Hz; Stress, 28 cells, 4.17 ± 0.41 Hz; $t_{76} = 0.047$, $p = 0.937$; Fig. 1E) and burst activity of these neurons. (Naïve, 50 cells, 36.46 ± 3.96% burst; Stress, 28 cells, 41.77 ± 5.82%burst; $U = 624$, $p = 0.43$; Fig. 1F). The effect of stress was evaluated on circuit plasticity of vHIP-NAC shell (fimbria HFS on NAc shell monosynaptically-evoked spike discharge). During baseline, no difference was observed for current intensity (Naïve, $n = 6$, 0.42 ± 0.095 mA; Stress, $n = 7$, 0.71 ± 0.13 mA; $t_{11} = 1.74$, $p = 0.11$; Fig. 1G), basal spike probability (Naïve, $n = 6$, 0.49 ± 0.05; Stress, $n = 7$, 0.51 ± 0.03; $t_{11} = 0.33$, $p = 0.75$; Fig. 1H) and Latency (Naïve, $n = 6$, 21.58 ± 0.33 ms; Stress, $n = 7$, 20.26 ± 0.63 ms; $t_{11} = 1.76$, $p = 0.11$; Fig. 1I). After fimbria HFS, there was a change in evoked spike probability (Fig. 1J; $f = 2.47$) with respect to condition (naïve or stressed; $F_{1,11} = 68.7$, $p < 0.0001$) and time ($F_{7,77} = 3.47$, $p = 0.0028$) with interaction between factors (Condition × Time, $F_{7,77} = 43.25$, $p < 0.0001$). Stress produced a marked decrease in the mean % change in fimbria-evoked spike probability (Naïve, $n = 6$, 73.81 ± 14.67; Stress, $n = 7$, −67.33 ± 7.97; $t_{11} = 8.81$, $p < 0.0001$; $d = 4.79$; Fig. 1K),

RE inactivation reverses the increased immobility induced by stress

The surgery to implant a guide cannulate targeting the RE was performed one day after the end of the stress protocol and the rats were subjected to the FST 1–2 weeks later (Naïve-Veh, $n = 6$; Naïve-TTX, $n = 5$; Stress-Veh, $n = 7$; Stress-TTX, $n = 8$; Fig. 2A). TTX was infused into the RE 10 min before the animal was subjected to the FST (Fig. 2A, B; Schematic representation of RE injection placements in Supplementary Fig. 2). No effect of stress exposure and RE inactivation was found for the latency to immobility (Naïve-Veh, 150.8 ± 18.92 s; Naïve-TTX, 141.4 ± 30.59 s; Stress-Veh, 114.3 ± 17.41 s; Stress-TTX, 174.1 ± 16.86 s; Stress: $F_{1,22} = 0.009$, $p = 0.93$; treatment: $F_{1,22} = 1.52$, $p = 0.23$; interaction: $F_{1,22} = 2.86$, $p = 0.10$; two-way ANOVA; Fig. 2C). However, the stress-induced increased immobility in the FST was reversed by inactivation of the RE with TTX (Naïve-Veh, 43.5 ± 5.67 s; Naïve-TTX, 41.6 ± 6.34 s; Stress-Veh, 78.14 ± 10.33 s; Stress-TTX, 39.5 ± 5.01 s; Stress: $F_{1,31} = 14.54$, $p = 0.0006$; treatment: $F_{2,31} = 7.44$, $p = 0.011$; interaction: $F_{2,31} = 4.46$, $p = 0.02$; 2-way ANOVA; $f = 0.95$; Fig. 2D).

In cases in which the TTX was administered outside of the RE boundaries (TTX/OUT), there was no impact of TTX administration on the factors measured in the FST (Latency: Stress-TTX/OUT, 111.0 ± 16.66 s; Naïve-Veh × Stress-TTX/OUT, $t_9 = 1.55$, $p = 0.16$, *t*-test; Immobility: Stress-TTX/OUT, Stress-TTX/OUT, 75.6 ± 8.00 s; Naïve-Veh × Stress-TTX/OUT, $t_9 = 3.357$, $p = 0.008$, $d = 2.03$).

Inactivation of the RE reverses the stress-induced hypodopaminergic state in the VTA

TTX was injected into the RE 10 min before recording VTA DA neurons (Fig. 3A; Schematic representation of RE injection placements is in the Supplementary Fig. 3). Representative photomicrographs showing the site of VTA recording and RE injection are shown in Fig. 3B, C, respectively. RE inactivation with TTX reversed the decrease in the number of spontaneously active VTA DA neurons induced by stress to control levels (Naïve-Veh, $n = 9$ rats, 63 cells, 1.09 ± 0.08 cells/track; Naïve-TTX, $n = 9$ rats, 59 cells, 1.09 ± 0.6 cells/track; Stress-Veh, $n = 9$, 37 cells, 0.6 ± 0.04 cells/track; Stress-TTX, $n = 7$ rats, 57 cells, 1.18 ± 0.08 cells/track; stress: $F_{1,30} = 8.98$, $p < 0.001$; treatment: $F_{1,30} = 19.47$, $p = 0.005$; interaction: $F_{1,30} = 19.01$, $p < 0.001$; two-way ANOVA; $f = 1.23$; Fig. 3D). No effect on firing rate (Naïve-Veh, 4.21 ± 0.31 Hz; Naïve-TTX, 3.53 ± 0.31 Hz; Stress-Veh, 3.08 ± 0.33 Hz; Stress-TTX, 3.45 ± 0.36 Hz; stress: $F_{1,213} = 3.64$, $p = 0.053$; treatment: $F_{1,213} = 0.32$, $p = 0.57$; interaction: $F_{1,213} = 2.21$, $p = 0.14$; 2-way ANOVA; Fig. 3E). An effect on burst activity was found (Naïve-Veh, 34.92 ± 3.44% burst; Naïve-TTX, 24.76 ± 3.71% burst; Stress-Veh, 22.11 ± 3.93% burst; Stress-TTX, 27.61 ± 3.84% burst; Kruskal-Wallis, $H = 7.94$, $p = 0.047$). However, Dunn's multiple comparisons did not demonstrate any difference between the groups (Fig. 3F).

The administration of TTX outside of the RE boundaries (TTX/OUT) did not impact number of active DA cells (Stress-TTX/OUT, $n = 3$, 0.61 ± 0.15 cells/track; Naïve-Veh × Stress-TTX/OUT, $t_{10} = 2.88$, $p = 0.02$, Effect size, $d = 1.912$), firing rate (Stress-TTX/OUT, 3.43 ± 0.66 Hz; Naïve-Veh × Stress-TTX/OUT, $t_{72} = 0.99$, $p = 0{,}32$) and burst activity (Stress-TTX/OUT, 27.1 ± 8.13% burst; Naïve-Veh × Stress-TTX/OUT, $U = 298$, $p = 0.47$, Mann-Whitney).

Inactivation of the RE partially rescues long-term potentiation in the NAc shell induced by vHIP stimulation in stressed rats

The effect of vHIP (fimbria) HFS on NAc shell monosynaptically-evoked spike discharge was assessed 1–2 weeks post-stress (Fig. 4A–C; Schematic representation of recording and stimulation placements in Supplementary Fig. 4A, B). TTX infusion into the RE was performed 10 min after the beginning of baseline recording (Naïve-Veh, $n = 6$; Naïve-TTX, $n = 5$; Stress-Veh, $n = 6$; Stress-TTX, $n = 6$; Stress-TTX/OUT, $n = 4$; Schematic representation of RE injections placements is in Supplementary Fig. 4C). The baseline recording was maintained for an additional 10 min after TTX injection and was followed by fimbria HFS. During the baseline period, no change in spike probability was observed after TTX injection in the RE in naïve and stressed rats ($p > 0.05$; 2-way ANOVA; Supplementary Fig. 5). At the post-injection baseline period, no significant difference was observed for current intensity and basal spike probability across the groups (Basal spike probability: Naïve-Veh, 0.45 ± 0.03; Naïve-TTX, 0.51 ± 0.07; Stress-Veh, 0.55 ± 0.06; Stress-TTX, 0.42 ± 0.06; Stress, $F_{1,19} = 0.018$, $p = 0.89$; Treatment, $F_{1,19} = 0.38$, $p = 0.54$; Interaction, $F_{1,19} = 2.45$, $p = 0.13$; 2-Way ANOVA; Fig. 4D; Current Intensity: Naïve-Veh, 0.37 ± 0.12; Naïve-TTX, 0.31 ± 0.04; Stress-Veh, 0.63 ± 0.28; Stress-TTX, 0.72 ± 0.22; Stress, $F_{1,19} = 2.85$, $p = 0.11$; Treatment, $F_{1,19} = 0.008$, $p = 0.93$; Interaction, $F_{1,19} = 0.16$, $p = 0.69$; 2-Way ANOVA; Fig. 4E). For latency, a significant effect of treatment and condition

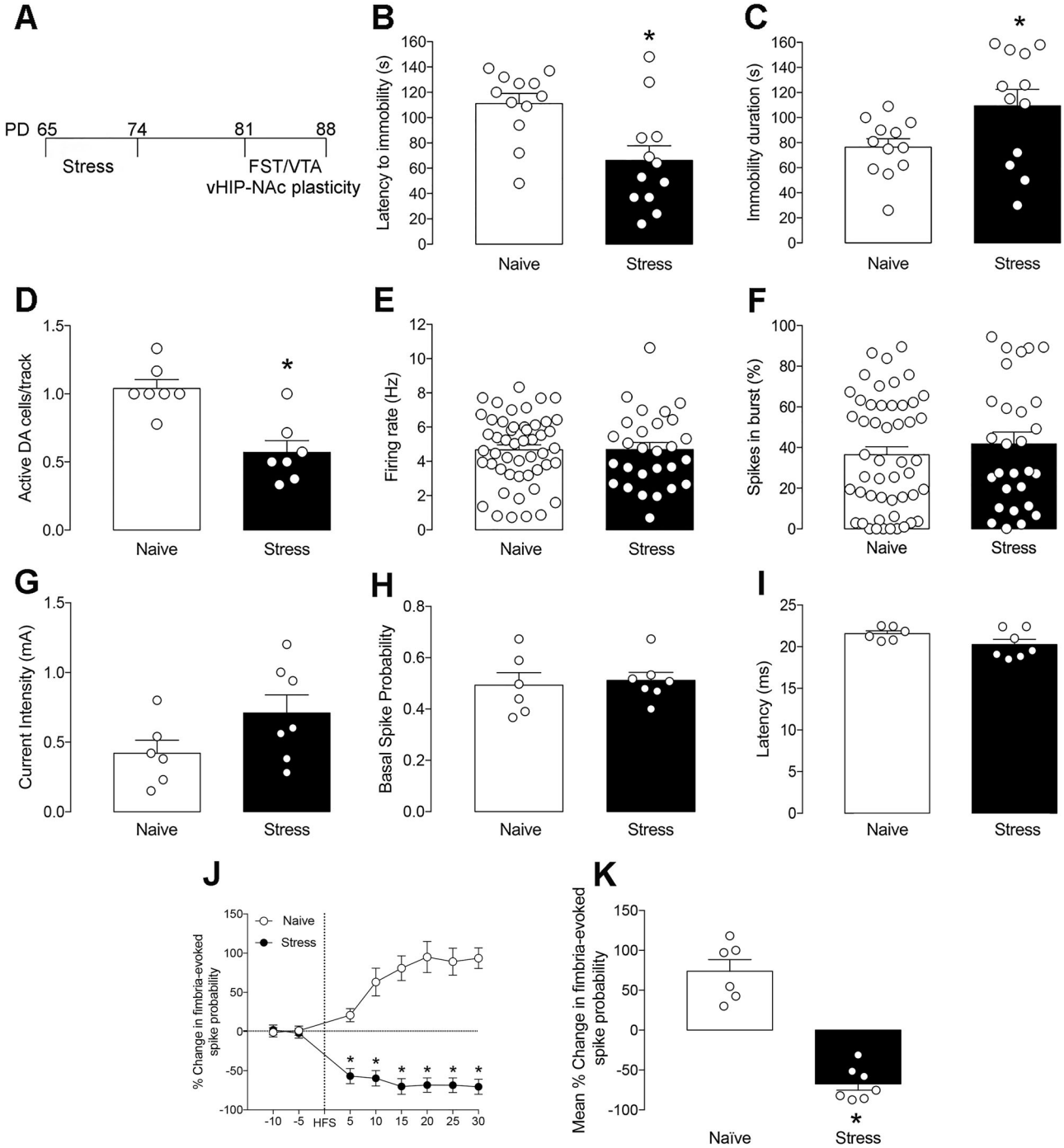

Fig. 1 Stress induces affective dysregulation and VTA hypodopaminergic states. A The rats were exposed to a 10-day stress protocol and subjected to FST and VTA recording 1–2 weeks later. Exposure to stress decreased the latency to immobility (**B**) and increased the immobility duration (**C**). Stressed rats showed downregulation of spontaneous active DA neurons (**D**) with no changes in firing rate (**E**) and % of spikes in bursts (**F**). For vHIP-Nac plasticity, stress did not affect current intensity (**G**), basal spike probability (H), and latency (**I**). Decreased % change was observed in stress animals (**J**: time-course; K: Mean). FST: Naïve, $n = 12$; Stress, $n = 12$. DA: Naïve, $n = 7$; Stress, $n = 7$. vHIP-NAc: Naïve, $n = 6$; Stress, $n = 7$. $^*p < 0.05$, *t*-test.

interaction was observed, with Stress-Vehicle group differing from Naïve-Vehicle (Naïve-Veh, 24.64 ± 1.05; Naïve-TTX, 23.19 ± 1.71; Stress-Veh, 20.06 ± 0.62; Stress-TTX, 23.52 ± 1.22; Stress, $F_{1,19} = 3.31$, $p = 0.08$; Treatment, $F_{1,19} = 0.80$, $p = 0.4$; Interaction, $F_{1,19} = 4.42$, $p = 0.049$; 2-Way ANOVA; $f = 0.64$; Fig. 4F). After fimbria HFS, % change of spike probability in NAc differed with regard to condition (naïve or stressed; $F_{1,19} = 25.88$, $p < 0.001$), time ($F_{9,171} = 3.71$, $p = 0.02$), but not for treatment (Veh or TTX; $F_{1,19} = 0.89$, $p > 0.05$). Significant interactions were found between factors (condition × treatment, $F_{1,19} = 15.01$, $p = 0.001$; time × condition, $F_{9,171} = 13.44$, $p < 0.001$; time × condition × treatment, $F_{9,171} = 8.99$, $p < 0.001$; three-way ANOVA; $f = 1.63$), but no interaction for time × treatment ($F_{9,171} = 1.37$, $p > 0.05$). Post-hoc analyses indicated that fimbria HFS increased the probability of evoking spikes in NAc shell neurons of naive animals and decreased the spike probability in stressed rats (Fig. 4G), similar to that reported

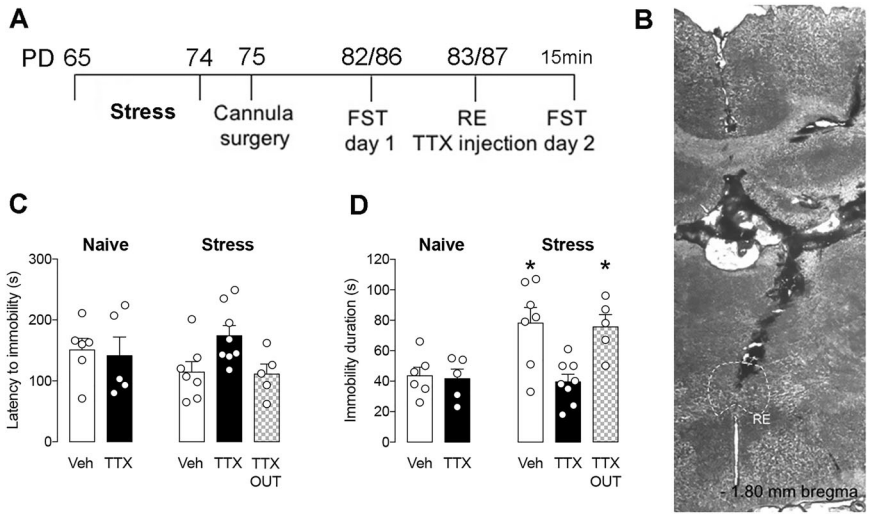

Fig. 2 RE inactivation reversed the increased immobility in FST induced by stress. A Rats were anesthetized and implanted with a cannula in the RE 1 day following the stress protocol and were tested in the FST after 1 week. **B** Photograph of the microinjection site in the RE. **C** Latency to immobility was not affected by stress and RE inactivation. **D** RE inactivation prevented the increased immobility duration induced by stress. Naïve-Veh, $n = 6$; Naïve-TTX, $n = 5$; Stress-Veh, $n = 7$; Stress-TTX, $n = 8$; TTX injections that missed RE (Stress-TTX/OUT), $n = 5$. *$p < 0.05$ vs. naïve-vehicle, ANOVA.

previously [26]. TTX injection into the RE attenuated the increased spike probability in NAc shell after fimbria HFS in naive rats and partially reversed the decreased spike probability in the stressed group (baseline evoked-spike probability 30 min post-HFS: vehicle-treated naïve animals, 0.81 ± 0.04; vehicle-treated stressed animals 0.14 ± 0.06). RE inactivation reversed stress-induced deficits in vHIP-NAc synaptic plasticity (baseline evoked spike probability in TTX-treated stressed rats was 0.42 ± 0.06 and changed slightly to 0.43 ± 0.07 30 min post-HFS). The repeated stress protocol induced a marked decrease in the mean % change in fimbria-evoked spike probability, which was ameliorated with RE inactivation (Naïve-Veh, 82.44 ± 7.76; Naïve-TTX, 33.36 ± 13.17; Stress-Veh, −75.29 ± 9.53; Stress-TTX, 14.04 ± 29.06; $F_{1,19} = 25.63$, $p < 0.001$; treatment: $F_{1,19} = 1.34$, $p > 0.05$; interaction: $F_{1,19} = 15.51$, $p < 0.001$; 2-way ANOVA; $f = 1.64$; Fig. 4H), indicating that the RE may play a role in the disrupted vHIP-NAc plasticity following stress. Post-hoc analysis indicated that the mean % change in fimbria-evoked spike probability is higher in naïve animals ($p < 0.05$ vs. naïve-TTX, stress-Veh, stress-TTX; Tukey).

The administration of TTX outside of the RE boundaries (TTX/OUT) did not impact basal spike probability (Stress-TTX/OUT, 0.52 ± 0.06; Naïve-Veh x Stress-TTX/OUT, $t_8 = 1.10$, $p = 0.30$), current intensity (Stress-TTX/OUT, 0.73 ± 0.17; Naïve-Veh × Stress-TTX/OUT, $t_8 = 1.75$, $p = 0.12$), latency (Stress-TTX/OUT, 20.8 ± 0.94; Naïve-Veh × Stress-TTX/OUT, $t_8 = 2.54$, $p = 0.0.034$; $d = 1.64$), % Change (Naïve-Veh × Stress-TTX/OUT, Time, $F_{9,72} = 2.58$, $p = 0.012$; Condition/treatment, $F_{1,8} = 90.63$, $p = <0.0001$; Interaction, $F_{9,72} = 35.34$, $p < 0.0001$), and Mean % of change (Stress-TTX/OUT, −57.29 ± 10.74; Naïve-Veh × Stress-TTX/OUT, $t_8 = 10.84$, $p < 0.0001$, t-test, $d = 7.00$).

DISCUSSION

Repeated stress applied to adult rats induces behavioral and electrophysiological changes as indicated by increased immobility in the FST and a hypodopaminergic state in the VTA. These changes were reversed by RE inactivation. Moreover, stress exposure induced long-term depression (LTD) in vHIP-NAc plasticity, in which HFS typically produces early long-term potentiation (e-LTP) in normal rats. Although the RE inactivation in naïve rats slightly attenuated the NAc e-LTP induced by fimbria stimulation, in stressed rats the vHIP-NAc plasticity disruption was partially reversed by inactivation of the RE. These findings support the role of the RE in affective dysregulation and VTA DA activity induced by repeated adult stress.

The exposure of rodents to repeated stress has been used extensively to model behavioral and physiological aspects of psychiatric disorders, including depression [47–50]. Models such as chronic mild stress and repeated chronic stressors induce amotivational states which can be reflected by increased immobility time in the FST [19, 20, 51]. Similarly, we found that rats subjected to repeated stress presented increased immobility time and decreased latency to immobility. Evidence indicates that affective dysregulation observed in rodents is accompanied by a hypodopaminergic state [23, 51]. As reported previously [23], the stress procedure used here blunted VTA DA neuron population activity. This hypodopaminergic state is consistent with previous literature showing that stress-inducing disruption in motivational behavior is linked with dopaminergic activity downregulation [25, 26, 51–55]. Moreover, in clinic depression, disrupted dopaminergic activity in areas associated with reward response has been described [16–18].

The affective dysregulation observed in stress-based models strongly affects the anatomy and activity of the PFC and vHIP [56–63] and it is associated with MDD [64]. These areas and their intrinsic connectivity are essential for stress coping and are linked to affective dysregulation in which their dysfunction can be associated with poor stress outcomes [58, 65–68]. The RE is a brain area related to HIP-PFC connectivity [1, 2, 5] which is involved in the regulation of a variety of behaviors, such as fear responses, passive avoidance, motivation, and working memory [14, 69–77]. In addition, the RE was described recently to be involved in the affective dysregulation induced by stress exposure [14]. Prior lesion of the RE prevented the behavioral changes and dendritic PFC and HIP atrophy induced by CMS [14, 15]. Our data support the role of RE inactivation in reversing the impact of stress exposure on motivational responses. As described previously, the repeated stress regimen increases the immobility in the FST, which was normalized by RE inactivation performed prior to the test. Also, TTX-induced inactivation of the RE did not affect the immobility response of naïve rats. These data are not consistent with the decreased immobility in RE lesioned naïve animals reported by others [14], which could be due to the potential for adaptive changes [78] following the lesion of the RE prior to both FST exposures instead of selective inactivation performed before the test phase in our study. One potential caveat in our study relates to the

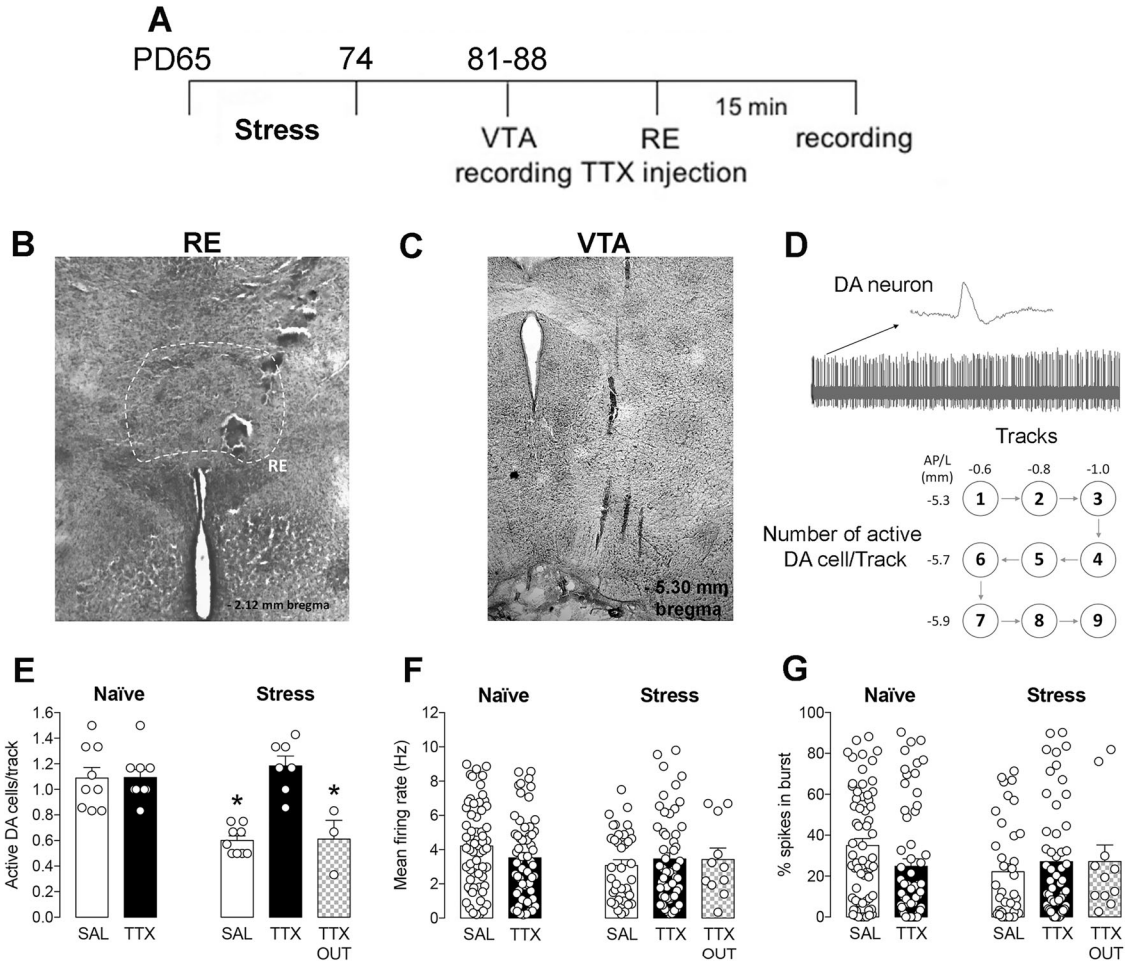

Fig. 3 RE inactivation rescues the hypodopaminergic state in the VTA induced by stress exposure. A Rats underwent VTA recording 1–2 weeks after the stress procedure termination. Representative photomicrographs of RE injection (**B**) and recording electrodes in the VTA placements (**C**). **D** Identified DA neurons were recorded in the VTA in a well-characterized grid pattern to assess the number of active DA neurons in each track. RE inactivation rescued the downregulation of active DA neurons/track (**E**) but did not impact the firing rate (**F**) and % spikes in burst (**G**). Naïve-Veh, $n = 9$; Naïve-TTX, $n = 9$; Stress-Veh, $n = 9$; Stress-TTX, $n = 7$; Stress-TTX/OUT, $n = 3$. $^*p < 0.05$ vs. naïve-vehicle, ANOVA.

finding that surgical cannula implantation appeared to alter the immobility latency in the FST. Stress has been described to upregulate several inflammatory markers in the brain, including COX-2 [79]. Since surgery took place 24 h after stress, the injection of postoperative carprofen (COX-2 inhibitor) could have potentially impacted the stress-induced FST latency measure. Nonetheless, these data still support the role of RE regulating motivation and underlying the stress outcomes observed here.

Impairment of affective response typically is accompanied by downregulation of dopaminergic activity in the VTA [25, 26, 51, 52, 54]. In our study, the animals subjected to the stress procedure presented a decreased number of spontaneously active DA neurons in the VTA, which was normalized by previous RE inactivation. In fact, the RE represents a key node in modulating the circuit involved in the regulation of dopaminergic activity [3]. It was shown previously that activation of RE increases the number of active DA neurons in the VTA which is prevented by vHIP inactivation. Also, the hyperdopaminergic state induced by the inactivation of ilPFC is driven by RE activity, reflecting the role of RE as a node between HIP and PFC in terms of regulating dopaminergic neuron activity. While these previous studies demonstrate that RE modulates dopaminergic activity indirectly through vHIP, RE does have sparse direct projections to VTA [5]. However, given our data that vHIP inactivation prevents the effect of RE on the VTA, and that VTA population activity is dependent on the ventral pallidum (VP) [80], we propose that the RE modulation of VTA activity observed here involves the vHIP, as the RE-HIP connectivity appears to be anatomically and functionally more relevant [3, 5]. Altogether, the direct projection might be affecting the firing rate but would not impact population activity. The present data support the role of RE in dopaminergic activity regulation and provides additional information in relation to stress-dependent RE modulation of DA function, suggesting the engagement of RE in the hypodopaminergic state. However, the recordings of VTA DA neurons were performed in anesthetized animals, which could potentially impact the results. Nonetheless, this approach was used since population activity metrics cannot be assessed in awake animals [44, 45]. Furthermore, results using this approach have been shown to be highly correlated with behavior [21, 27] and therefore is likely to be relevant to the behavioral outcomes observed here.

An important pathway involved in the modulation of dopaminergic activity and affective dysregulation is the vHIP-NAc projection [21, 26, 32]. The ventral subiculum of the hippocampus (vSub) regulates contextual information of behaviors and stress responses [81]. The NAc has been extensively implicated in reward responses [22, 82], as has its connectivity with the vHIP [30]. As described above, the RE represents an important node of

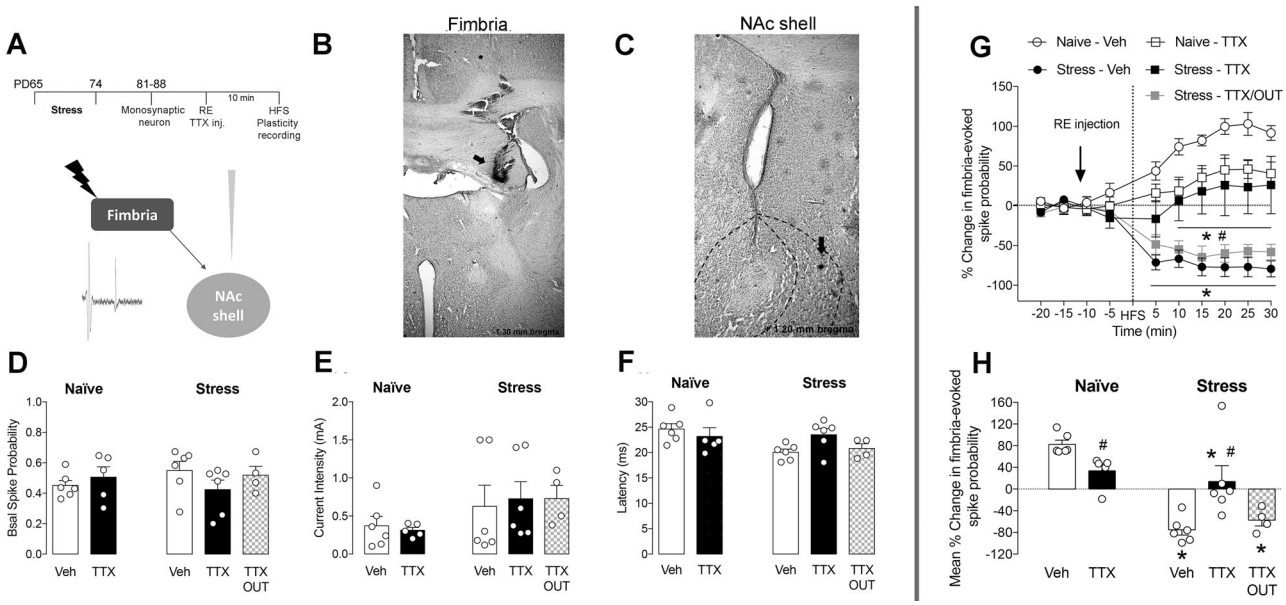

Fig. 4 RE inactivation partially rescues the impaired vHIP-NAc synaptic plasticity induced by stress exposure. 1–2 weeks following the stress exposure, monosynaptic connectivity between vHIP and NAc shell was evaluated. **A** A recording electrode was placed in the NAC shell and vHIP projections (fimbria) were electrically stimulated. Representative photomicrographs of sites of fimbria stimulation (**B**) and recording electrode placement in the NAc shell (**C**). Baseline values of spike probability (**D**) and current intensity (**E**) were not affected by stress and TTX injection in the RE. **F** Evoked spike latency was decreased in the stress-vehicle group compared to naïve-vehicle (*p < 0.05, ANOVA). Time-course of % change in fimbria-evoked spike probability (**G**) and the mean values of % change in fimbria-evoked spike probability (**H**). HFS of the fimbria induced e-LTP in naïve-vehicle rats which were impaired by stress showing a LTD form of plasticity. RE inactivation partially rescued the e-LTP plasticity form of vHIP-Nac shell connectivity and attenuated the e-LTP in naïve animals (*$p < 0.05$ to naïve-vehicle, #$p < 0.05$ to stress-vehicle, ANOVA). Naïve-Veh, $n = 6$; Naïve-TTX, $n = 5$; Stress-Veh, $n = 6$; Stress-TTX, $n = 6$; Stress-TTX/OUT, $n = 4$.

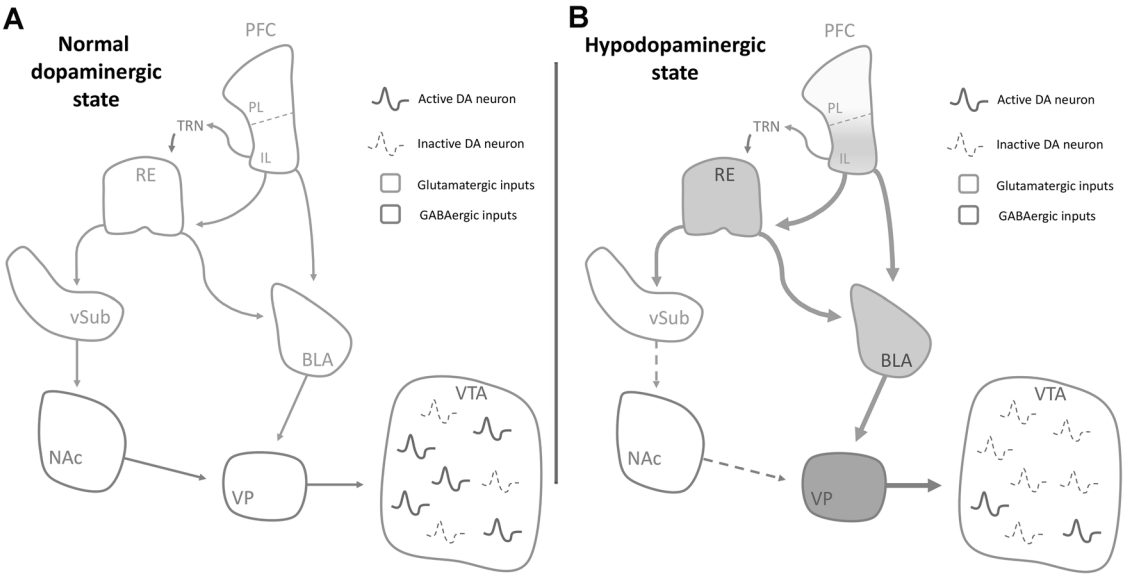

Fig. 5 A hypothetical circuit model mediating stress-induced hypodopaminergic state and affective dysregulation. A Normal relationship and interconnections among mPFC, RE, vSub, BLA and NAc-VP-VTA pathway. **B** Stress exposure alters the relationship among these systems. Stress exposure is proposed to facilitate the excitatory projection from the iIPFC to BLA and directly and indirectly to the RE. Enhanced activity of RE would induce vHIP dysfunction and decrease its connectivity with the NAc, thereby attenuating NAc activation. The impairment of NAc activation would then disinhibit the VP which sends inhibitory projection to the VTA. VP activity is also driven by BLA inputs and RE could induce more activation of the BLA. Ultimately, the BLA excitability, RE activity, and vHIP-NAc dysfunction can contribute to the downregulation of dopaminergic activity in VTA and affective dysregulation.

regulation of dopaminergic activity via the vHIP as well as an integrator of PFC outputs [3]. Thus, disruption of the hippocampus, the NAc, and their connectivity may underlie the responses to repeated stress. It has been reported that chronic stress impairs e-LTP in the vHIP-NAc pathway and decreases sucrose preference [30]. Also, we found previously that animals showing helpless behavior present a vSub-NAc shell pathway disruption and e-LTD instead of the e-LTP observed in naïve and nonhelpless rats [26]. Our data point to similar impairments in vSub-NAc shell plasticity induced by repeated stress. The inability of the vSub to induce

facilitatory plasticity in the NAc may accentuate the hypodopaminergic state observed after stress [21]. Moreover, other factors can influence the ability of the NAc to respond to stimuli, such as neuromodulation by DA [83]. For example, neurons expressing D1 and D2 receptors could respond differently to the stimulus. We did not consider the cell-type specificity in the analysis due to previous data showing that the stimulation of hippocampus projection to NAc shell induces increased excitatory postsynaptic potentials which is attenuated by D1 but not D2 activation [84]. Thus, it is likely that the effect of DA over NAc activity after fimbria HFS in stress conditions may be influenced by D1 rather than D2 receptors either located postsynaptically or presynaptically [85].

We investigated the influence of RE in the vSub-NAc plasticity, considering its role in regulating dopaminergic activity through the HIP [3]. Our data demonstrated that the effect of RE inactivation on the vSub-NAc pathway was condition-dependent. Thus, in naïve animals, RE inactivation attenuated the e-LTP in NAc shell after vSub projection (fimbria) HFS. On the other hand, in stressed rats, RE inactivation partially normalized the induction of e-LTP in the NAc shell. These data suggest that the vSub-NAc disruption induced by stress is in part regulated by RE activity. However, other brain areas also may play a role in the changes induced by stress and are also likely influenced by the RE, such as the basolateral amygdala (BLA) [33, 71]. In affective dysregulation, hyperexcitability of the BLA has been reported [21, 52, 53] in which BLA-vHIP projections can lead to disruption of vHIP outputs. Indeed, the adult repeated stress protocol increases BLA activity and disrupt its connectivity [39]. Therefore, the vSub-NAc dysregulation observed in the stress group may result from the combined influence of RE and BLA activity. Thus, the RE is likely part of a broad circuit involved in the modulation of dopaminergic activity. The RE projections to vHIP are proposed to be glutamatergic, as the NMDA activation changes VTA DA activity [3]. The vHIP activation is likely increasing the excitatory drive to the NAc shell which is a GABAergic nucleus. The inhibitory transmission originating from NAc to ventral pallidum (VP) increases DA neuron excitability in the VTA [27]. In the case of hypodopaminergic states as observed here, RE projections seem to contribute to the disruption of vHIP excitatory projections to GABAergic cells in the NAc shell which produce less engagement of inhibitory transmission innervating the VP. The resultant VP disinhibition would thereby increase the inhibitory drive of the VTA and ultimately lead to downregulated dopaminergic activity (Fig. 5) [21].

In conclusion, our findings support the role of the RE in the regulation of affective dysregulation and blunted VTA DA function induced by adult repeated stress. Also, it points to the NAc and HIP as a potential neural circuit in which the RE modulates the behavioral and VTA DA neuron activity changes occurring after stress. Therefore, the RE may represent a key brain region involved in the neurobiology of amotivational states and may provide insights on circuit dysfunction of the maladaptive stress response.

REFERENCES

1. Vertes RP. Analysis of projections from the medial prefrontal cortex to the thalamus in the rat, with emphasis on nucleus reuniens. J Comp Neurol. 2002;442:163–87.
2. Di Prisco GV, Vertes RP. Excitatory actions of the ventral midline thalamus (rhomboid/reuniens) on the medial prefrontal cortex in the rat. Synapse. 2006;60:45–55.
3. Zimmerman EC, Grace AA. The nucleus reuniens of the midline thalamus gates prefrontal-hippocampal modulation of ventral tegmental area dopamine neuron activity. J Soc Neurosci. 2016;36:8977–84.
4. Zhang Y, Yoshida T, Katz DB, Lisman JE. NMDAR antagonist action in thalamus imposes δ oscillations on the hippocampus. J Neurophysiol. 2012;107:3181–9.
5. Herkenham M. The connections of the nucleus reuniens thalami: evidence for a direct thalamo-hippocampal pathway in the rat. J Comp Neurol. 1978;177:589–610.
6. Small SA, Schobel SA, Buxton RB, Witter MP, Barnes CA. A pathophysiological framework of hippocampal dysfunction in ageing and disease. Nat Rev Neurosci. 2011;12:585–601.
7. Godsil BP, Kiss JP, Spedding M, Jay TM. The hippocampal–prefrontal pathway: the weak link in psychiatric disorders? Eur Neuropsychopharmacol. 2013;23:1165–81.
8. Dolleman-van der Weel MJ, Witter MP. The thalamic midline nucleus reuniens: potential relevance for schizophrenia and epilepsy. Neurosci Biobehav Rev. 2020;119:422–39.
9. Sheline YI, Barch DM, Price JL, Rundle MM, Vaishnavi SN, Snyder AZ, et al. The default mode network and self-referential processes in depression. Proc Natl Acad Sci USA. 2009;106:1942–7.
10. Goveas J, Xie C, Wu Z, Douglas Ward B, Li W, Franczak MB, et al. Neural correlates of the interactive relationship between memory deficits and depressive symptoms in nondemented elderly: resting fMRI study. Behav Brain Res. 2011;219:205–12.
11. Sheline YI, Wang PW, Gado MH, Csernansky JG, Vannier MW. Hippocampal atrophy in recurrent major depression. Proc Natl Acad Sci USA. 1996;93:3908–13.
12. Drevets WC, Price JL, Simpson JR, Todd RD, Reich T, Vannier M, et al. Subgenual prefrontal cortex abnormalities in mood disorders. Nature. 1997;386:824–7.
13. Oliveira JF, Dias NS, Correia M, Gama-Pereira F, Sardinha VM, Lima A, et al. Chronic stress disrupts neural coherence between cortico-limbic structures. Front Neural Circuits. 2013;7:10.
14. Kafetzopoulos V, Kokras N, Sotiropoulos I, Oliveira JF, Leite-Almeida H, Vasalou A, et al. The nucleus reuniens: a key node in the neurocircuitry of stress and depression. Mol Psychiatry. 2018;23:579–86.
15. Kafetzopoulos V, Kokras N, Sousa N, Antoniou K, Sotiropoulos I, Dalla C. Nucleus reuniens lesion and antidepressant treatment prevent hippocampal neurostructural alterations induced by chronic mild stress in male rats. Neuroscience. 2021;454:85–93.
16. Lambert G, Johansson M, Agren H, Friberg P. Reduced brain norepinephrine and dopamine release in treatment-refractory depressive illness: evidence in support of the catecholamine hypothesis of mood disorders. Arch Gen Psychiatry. 2000;57:787–93.
17. Nestler EJ, Carlezon WA. The mesolimbic dopamine reward circuit in depression. Biol Psychiatry. 2006;59:1151–9.
18. Reddy PL, Khanna S, Subhash MN, Channabasavanna SM, Rao BS. CSF amine metabolites in depression. Biol Psychiatry. 1992;31:112–8.
19. Czéh B, Fuchs E, Wiborg O, Simon M. Animal models of major depression and their clinical implications. Prog Neuropsychopharmacol Biol Psychiatry. 2016;64:293–310.
20. Muir J, Lopez J, Bagot RC. Wiring the depressed brain: optogenetic and chemogenetic circuit interrogation in animal models of depression. Neuropsychopharmacology. 2018. https://doi.org/10.1038/s41386-018-0291-6.
21. Belujon P, Grace AA. Dopamine system dysregulation in major depressive disorders. Int J Neuropsychopharmacol. 2017;20:1036–46.
22. Wise RA. Dopamine and reward: the anhedonia hypothesis 30 years on. Neurotox Res. 2008;14:169–83.
23. Gomes FV, Zhu X, Grace AA. The pathophysiological impact of stress on the dopamine system is dependent on the state of the critical period of vulnerability. Mol Psychiatry. 2019. 2019. https://doi.org/10.1038/s41380-019-0514-1.
24. Patton MH, Bizup BT, Grace AA. The infralimbic cortex bidirectionally modulates mesolimbic dopamine neuron activity via distinct neural pathways. J Neurosci. 2013;33:16865–73.
25. Moreines JL, Owrutsky ZL, Grace AA. Involvement of infralimbic prefrontal cortex but not lateral habenula in dopamine attenuation after chronic mild stress. Neuropsychopharmacology. 2017;42:904–13.
26. Belujon P, Grace AA. Restoring mood balance in depression: ketamine reverses deficit in dopamine-dependent synaptic plasticity. Biol Psychiatry. 2014;76:927–36.
27. Grace AA. Dysregulation of the dopamine system in the pathophysiology of schizophrenia and depression. Nat Rev Neurosci. 2016;17:524–32.
28. Floresco SB, Todd CL, Grace AA. Glutamatergic afferents from the hippocampus to the nucleus accumbens regulate activity of ventral tegmental area dopamine neurons. J Neurosci. 2001;21:4915–22.
29. Lodge DJ, Grace AA. The hippocampus modulates dopamine neuron responsivity by regulating the intensity of phasic neuron activation. Neuropsychopharmacology. 2006;31:1356–61.
30. LeGates TA, Kvarta MD, Tooley JR, Francis TC, Lobo MK, Creed MC, et al. Reward behaviour is regulated by the strength of hippocampus-nucleus accumbens synapses. Nature. 2018;564:258–62.
31. Bagot RC, Parise EM, Peña CJ, Zhang H-X, Maze I, Chaudhury D, et al. Ventral hippocampal afferents to the nucleus accumbens regulate susceptibility to depression. Nat Commun. 2015;6:7062.
32. Muir J, Tse YC, Iyer ES, Biris J, Cvetkovska V, Lopez J, et al. Ventral hippocampal afferents to nucleus accumbens encode both latent vulnerability and stress-induced susceptibility. Biol Psychiatry. 2020;88:843–54.
33. Vertes RP, Hoover WB, Do Valle AC, Sherman A, Rodriguez JJ. Efferent projections of reuniens and rhomboid nuclei of the thalamus in the rat. J Comp Neurol. 2006;499:768–96.

34. Klinger K, Gomes FV, Rincón-Cortés M, Grace AA. Female rats are resistant to the long-lasting neurobehavioral changes induced by adolescent stress exposure. Eur Neuropsychopharmacology. 2019;29:1127–37.
35. Bueno-Fernandez C, Perez-Rando M, Alcaide J, Coviello S, Sandi C, Castillo-Gómez E, et al. Long term effects of peripubertal stress on excitatory and inhibitory circuits in the prefrontal cortex of male and female mice. Neurobiol Stress. 2021;14:100322.
36. Wei J, Yuen EY, Liu W, Li X, Zhong P, Karatsoreos IN, et al. Estrogen protects against the detrimental effects of repeated stress on glutamatergic transmission and cognition. Mol Psychiatry. 2014;19:588–98.
37. Bale TL, Epperson CN. Sex differences and stress across the lifespan. Nat Neurosci. 2015;18:1413–20.
38. Seney ML, Sibille E. Sex differences in mood disorders: perspectives from humans and rodent models. Biol Sex Differ. 2014;5:17.
39. Uliana DL, Gomes FV, Grace AA. Stress impacts corticoamygdalar connectivity in an age-dependent manner. Neuropsychopharmacology. 2021;46:731–40.
40. Gomes FV, Grace AA. Prefrontal cortex dysfunction increases susceptibility to schizophrenia-like changes induced by adolescent stress exposure. Schizophr Bull. 2017;43:592–600.
41. Paxinos G, Watson C. The rat brain in stereotaxic coordinates. 3rd edition. San Diego: Academic Press; 1996.
42. Armario A. The forced swim test: Historical, conceptual and methodological considerations and its relationship with individual behavioral traits. Neurosci Biobehav Rev. 2021;128:74–86.
43. Porsolt RD, Le Pichon M, Jalfre M. Depression: a new animal model sensitive to antidepressant treatments. Nature. 1977;266:730–2.
44. Grace AA, Bunney BS. Intracellular and extracellular electrophysiology of nigral dopaminergic neurons-1. Identif Charact Neurosci. 1983;10:301–15.
45. Ungless MA, Grace AA. Are you or aren't you? Challenges associated with physiologically identifying dopamine neurons. Trends Neurosci. 2012;35:422–30.
46. Rosenkranz JA, Grace AA. Dopamine attenuates prefrontal cortical suppression of sensory inputs to the basolateral amygdala of rats. J Neurosci.2001;21:4090–103.
47. Herbison CE, Allen K, Robinson M, Newnham J, Pennell C. The impact of life stress on adult depression and anxiety is dependent on gender and timing of exposure. Dev Psychopathol. 2017;29:1443–54.
48. Slavich GM, Sacher J. Stress, sex hormones, inflammation, and major depressive disorder: Extending Social Signal Transduction Theory of Depression to account for sex differences in mood disorders. Psychopharmacology. 2019;236:3063–79.
49. Kendler KS, Karkowski LM, Prescott CA. Causal relationship between stressful life events and the onset of major depression. Am J Psychiatry. 1999;156:837–41.
50. Mineur YS, Belzung C, Crusio WE. Effects of unpredictable chronic mild stress on anxiety and depression-like behavior in mice. Behav Brain Res. 2006;175:43–50.
51. Rincón-Cortés M, Grace AA. Sex-dependent effects of stress on immobility behavior and VTA dopamine neuron activity: modulation by ketamine. Int J Neuropsychopharmacol. 2017;20:823–32.
52. Chang C-H, Grace AA. Amygdala-ventral pallidum pathway decreases dopamine activity after chronic mild stress in rats. Biol Psychiatry. 2014;76:223–30.
53. Neves GA, Grace AA. α7 nicotinic receptor full agonist reverse basolateral amygdala hyperactivity and attenuation of dopaminergic neuron activity in rats exposed to chronic mild stress. Eur Neuropsychopharmacol J Eur Coll Neuropsychopharmacol. 2019;29:1343–53.
54. Uliana DL, Gomes FV, Grace AA. Prelimbic medial prefrontal cortex disruption during adolescence increases susceptibility to helpless behavior in adult rats. Eur Neuropsychopharmacol. 2020:S0924977X2030122X.
55. Tye KM, Mirzabekov JJ, Warden MR, Ferenczi EA, Tsai H-C, Finkelstein J, et al. Dopamine neurons modulate neural encoding and expression of depression-related behaviour. Nature. 2013;493:537–41.
56. Cerqueira JJ, Mailliet F, Almeida OFX, Jay TM, Sousa N. The prefrontal cortex as a key target of the maladaptive response to stress. J Soc Neurosci. 2007;27:2781–7.
57. Sousa N, Lukoyanov NV, Madeira MD, Almeida OF, Paula-Barbosa MM. Reorganization of the morphology of hippocampal neurites and synapses after stress-induced damage correlates with behavioral improvement. Neuroscience. 2000;97:253–66.
58. Dias-Ferreira E, Sousa JC, Melo I, Morgado P, Mesquita AR, Cerqueira JJ, et al. Chronic stress causes frontostriatal reorganization and affects decision-making. Science. 2009;325:621–5.
59. Radley JJ, Sisti HM, Hao J, Rocher AB, McCall T, Hof PR, et al. Chronic behavioral stress induces apical dendritic reorganization in pyramidal neurons of the medial prefrontal cortex. Neuroscience. 2004;125:1–6.
60. Radley J, Morilak D, Viau V, Campeau S. Chronic stress and brain plasticity: Mechanisms underlying adaptive and maladaptive changes and implications for stress-related CNS disorders. Neurosci Biobehav Rev. 2015;58:79–91.
61. Liu R-J, Aghajanian GK. Stress blunts serotonin- and hypocretin-evoked EPSCs in prefrontal cortex: role of corticosterone-mediated apical dendritic atrophy. Proc Natl Acad Sci USA. 2008;105:359–64.
62. McEwen BS. Neurobiological and systemic effects of chronic stress. Chronic Stress (Thousand Oaks). 2017;1:2470547017692328.
63. McEwen BS, Nasca C, Gray JD. Stress effects on neuronal structure: hippocampus, amygdala, and prefrontal cortex. Neuropsychopharmacol Publ Am Coll Neuropsychopharmacol. 2016;41:3–23.
64. Duman RS, Aghajanian GK. Synaptic dysfunction in depression: potential therapeutic targets. Science. 2012;338:68–72.
65. Banasr M, Sanacora G, Esterlis I. Macro- and microscale stress-associated alterations in brain structure: translational link with depression. Biol Psychiatry. 2021;90:118–27.
66. MacQueen G, Frodl T. The hippocampus in major depression: evidence for the convergence of the bench and bedside in psychiatric research? Mol Psychiatry. 2011;16:252–64.
67. Murray EA, Wise SP, Drevets WC. Localization of dysfunction in major depressive disorder: prefrontal cortex and amygdala. Biol Psychiatry. 2011;69:e43–54.
68. Davey CG, Yücel M, Allen NB. The emergence of depression in adolescence: development of the prefrontal cortex and the representation of reward. Neurosci Biobehav Rev. 2008;32:1–19.
69. Cassel J-C, Ferraris M, Quilichini P, Cholvin T, Boch L, Stephan A, et al. The reuniens and rhomboid nuclei of the thalamus: a crossroads for cognition-relevant information processing? Neurosci Biobehav Rev. 2021;126:338–60.
70. Griffin AL. The nucleus reuniens orchestrates prefrontal-hippocampal synchrony during spatial working memory. Neurosci Biobehav Rev. 2021;128:415–20.
71. Silva BA, Astori S, Burns AM, Heiser H, van den Heuvel L, Santoni G, et al. A thalamo-amygdalar circuit underlying the extinction of remote fear memories. Nat Neurosci. 2021;24:964–74.
72. Linley SB, Athanason AC, Rojas AKP, Vertes RP. Role of the reuniens and rhomboid thalamic nuclei in anxiety-like avoidance behavior in the rat. Hippocampus. 2021;31:756–69.
73. Xu W, Sudhof TC. A neural circuit for memory specificity and generalization. Science. 2013;339:1290–5.
74. Layfield DM, Patel M, Hallock H, Griffin AL. Inactivation of the nucleus reuniens/rhomboid causes a delay-dependent impairment of spatial working memory. Neurobiol Learn Mem. 2015;125:163–7.
75. Davoodi FG, Motamedi F, Akbari E, Ghanbarian E, Jila B. Effect of reversible inactivation of reuniens nucleus on memory processing in passive avoidance task. Behav Brain Res. 2011;221:1–6.
76. Hallock HL, Wang A, Griffin AL. Ventral midline thalamus is critical for hippocampal-prefrontal synchrony and spatial working memory. J Neurosci. 2016;36:8372–89.
77. Troyner F, Bertoglio LJ. Nucleus reuniens of the thalamus controls fear memory reconsolidation. Neurobiol Learn Mem. 2021;177:107343.
78. Vaidya AR, Pujara MS, Petrides M, Murray EA, Fellows LK. Lesion studies in contemporary neuroscience. Trends Cogn Sci. 2019;23:653–71.
79. Madrigal JLM, Moro MA, Lizasoain I, Lorenzo P, Fernández AP, Rodrigo J, et al. Induction of cyclooxygenase-2 accounts for restraint stress-induced oxidative status in rat brain. Neuropsychopharmacol Publ Am Coll Neuropsychopharmacol. 2003;28:1579–88.
80. Floresco SB, West AR, Ash B, Moore H, Grace AA. Afferent modulation of dopamine neuron firing differentially regulates tonic and phasic dopamine transmission. Nat Neurosci. 2003;6:968–73.
81. Herman JP, Mueller NK. Role of the ventral subiculum in stress integration. Behav Brain Res. 2006;174:215–24.
82. Lammel S, Lim BK, Malenka RC. Reward and aversion in a heterogeneous midbrain dopamine system. Neuropharmacology. 2014;76(Pt B):351–9.
83. Floresco SB, Blaha CD, Yang CR, Phillips AG. Modulation of hippocampal and amygdalar-evoked activity of nucleus accumbens neurons by dopamine: cellular mechanisms of input selection. J Neurosci. 2001;21:2851–60.
84. Charara A, Grace AA. Dopamine receptor subtypes selectively modulate excitatory afferents from the hippocampus and amygdala to rat nucleus accumbens neurons. Neuropsychopharmacol Publ Am Coll Neuropsychopharmacol. 2003;28:1412–21.
85. O'Donnell P, Grace AA. Tonic D2-mediated attenuation of cortical excitation in nucleus accumbens neurons recorded in vitro. Brain Res. 1994;634:105–12.

ACKNOWLEDGEMENTS

The authors wish to thank Niki MacMurdo for technical assistance and Loretta Liu for drawing assistance.

AUTHOR CONTRIBUTIONS

DLU: conceptualization, methodology, data acquisition, formal analysis, interpretation, writing—original draft. FVG: conceptualization, methodology, data acquisition, interpretation and writing—review & editing. AAG: conceptualization, resources, interpretation, writing—review & editing, supervision and funding acquisition.

FUNDING

This study was funded by US National Institutes of Health (NIH; MH57440 to AAG). FVG received a São Paulo Research Foundation Young Investigator grant (FAPESP – 2018/ 17597-3). AAG has received consulting fees from Alkermes, Lundbeck, Takeda, Roche, Lyra, Concert, and SynAgile and research funding from Lundbeck.

COMPETING INTERESTS

DLU and FVG declare no conflict of interest.

ADDITIONAL INFORMATION

Supplementary information The online version contains supplementary material available at https://doi.org/10.1038/s41386-022-01333-1.

Correspondence and requests for materials should be addressed to Daniela L. Uliana.

Reprints and permission information is available at http://www.nature.com/reprints

Publisher's note Springer Nature remains neutral with regard to jurisdictional claims in published maps and institutional affiliations.